Quaternion-based strap-down integration method for applications of inertial sensing to gait analysis

A. M. Sabatini

Scuola Superiore Sant'Anna, Pisa, Italy

Abstract—*The proposed strap-down integration method exploits the cyclical nature of human gait: during the gait swing phase, the quaternion-based attitude representation is integrated using a gyroscope from initial conditions that are determined during stance by an accelerometer. Positioning requires double time integration of the gravity-compensated accelerometer signals during swing. An interpolation technique applied to attitude quaternions was developed to improve the accuracy of orientation and positioning estimates by accounting for the effect of sensor bias and scale factor drifts. A simulation environment was developed for the analysis and testing of the proposed algorithm on a synthetic movement trajectory. The aim was to define the true attitude and positioning used in the computation of estimation errors. By thermal modelling, the changes of bias and scale factor of the inertial sensors, calibrated at a single reference temperature, were analysed over a range of* $\pm$ *10 °C, for measurement noise standard deviations up to* $\sigma_g = 2.5\,^\circ\,s^{-1}$ *(gyroscope) and* $\sigma_a = 0.05\ m\,s^{-2}$ *(accelerometer). The compensation technique reduced the maximum root mean square errors (RMSEs) to:* $RMSE_\theta = 14.6^\circ$ *(orientation) and* $RMSE_d = 17.7$ *cm (positioning) for an integration interval of one gait cycle (an improvement of 3° and 7 cm);* $RMSE_\theta = 14.8^\circ$ *and* $RMSE_d = 30.0$ *cm for an integration interval of two gait cycles (an improvement of 11° and 262 cm).*

Keywords—*Inertial sensing, Gait analysis, Strap-down integration, Quaternion of rotation, Computer simulations*

Med. Biol. Eng. Comput., 2005, **43**, 94–101

1 Introduction

INERTIAL SENSING is used to provide the information needed to estimate the attitude and positioning of rigid bodies relative to an absolute reference frame. Until recently, inertial sensing has been primarily applied in fields such as aerospace, because of the complexity and cost of the inertial measurement units (IMUs). The recent technological advance of micro electromechanical systems (MEMS) have substantially changed the situation, by introducing sensor devices, such as accelerometers and gyroscopes, that are characterised by their low cost, small size, light weight and limited power requirements. Nowadays, inertial sensing is thus of interest also to human movement scientists (OHTAKI *et al.*, 2001; MAYAGOITIA *et al.*, 2002), owing to the ability of IMU-based ambulatory monitoring systems to gather information about the manner in which humans perform motor activities in several contexts where the traditional approach to movement analysis may fail to operate properly (BUSSMANN *et al.*, 1995).

Recently, the use of both accelerometers and gyroscopes has been demonstrated for the assessment of gait features, including stride time and length. Stride time can be detected by searching for signal features, such as the sharp peaks that occur when the foot hits the ground (AMINIAN *et al.*, 1999; PAPPAS *et al.*, 2001). Usually, stride length is estimated by indirect methods that are based on biomechanical models, fed from the reconstructed angular rotations of body segments relative to the absolute space (MIYAZAKI, 1997; AMINIAN *et al.*, 2002). Alternatively, there exists the direct strap-down method: in this approach, the attitude of the rigid body and its non-gravitational accelerations are sensed by gyroscopes and accelerometers strapped to the body.

The co-ordinate transformation matrix required to take body-sensed measurements and to represent them in the absolute reference frame, the attitude matrix, is computed by time-integrating the signals from a triaxial gyroscope, once the initial conditions are available (attitude estimation). The attitude matrix also allows double time integration of the signals from triaxial accelerometer in the absolute reference frame without contamination by the gravity field, to which accelerometers are sensitive (positioning estimation). Owing to the influence of biases and sensitivity drifts, the time-integration processes can quickly build up errors from both inertial sensors.

A number of reports have been published regarding inertial sensing of human movement based on strap-down integration. The aim in LUINGE (2002) was to estimate the orientation vector of body segments during the execution of specific functional activities, i.e. crate-lifting tasks and eating routines.

Correspondence should be addressed to Professor Angelo M. Sabatini; email: a.sabatini@mail-arts.sssup.it

Paper received 15 March and in final form 19 July 2004

MBEC online number: 20053967

A Kalman filter was implemented to fuse the information obtained from an IMU composed of two triaxial sensors, i.e. one gyroscope and one accelerometer, with *a priori* information about the behaviour of the system of interest. The proposed method is appropriate if the magnitude of the acceleration can be neglected with respect to gravity: the validity of this assumption is dependent on the characteristics of the tracked movement. Moreover, as the signals of the accelerometer are not affected by a rotation around the vertical (heading), additional information is required to compensate for the heading drift.

In BACHMANN (2000), the IMU was composed of three triaxial sensors, one gyroscope, one accelerometer and one magnetometer. The aim was to track the movement of human limbs in real time by means of multiple inertial sensors for virtual-reality applications. The information from the accelerometer and the magnetometer was used to track the low-frequency components of the movement, and the information from the gyroscope was used to track the high-frequency components. A quaternion-based Kalman filter allowed continuous correction for drift and tracking of the movement through all orientations.

Another motion capture device is described in GUILLEMAUD *et al.* (2003), where the aim was to develop a wearable tool in the medical domain, for activity classification or monitoring. The IMU was composed of two triaxial sensors, i.e. one accelerometer and one magnetometer, the signals of which were fused to estimate the body orientation. Although suitable for tracking slow movements, this gyroscope-free method is not suited for fast movements, yielding quite large orientation errors during the movement. The data fusion technique is not described.

Crucial to the success of a strap-down approach is the development of efficient techniques to reduce the burden involved in the conventional methods for updating the attitude matrix (BORTZ, 1971). Most algorithms result in a twofold computing scheme: a specific attitude representation is updated periodically at a fast rate by integration of a vector differential equation; the attitude matrix is then updated at a slow rate. A number of techniques have been devised to represent the attitude of the rigid body, e.g. Euler angles and quaternions. Although it may suffer from problems of interpretation in terms of meaningful clinical or anatomical angles, the quaternion-based approach is of great practical interest, as it requires less computing time, gives better accuracy and avoids the singularity problems inherent in using Euler angles (CHOU, 1992; KIRTLEY, 2001): inertial sensing systems whose computations are based on Euler angles are unable to track orientation when a rigid body is in a vertical orientation, a serious limitation when tracking movements of human limb segments (BACHMANN, 2000).

In this paper, we have developed a quaternion-based filtering algorithm to estimate attitude and positioning by exploiting the information from an IMU composed of two triaxial sensors, one accelerometer and one gyroscope. The algorithm exploits the cyclical features of human walking for bias and sensitivity drift compensation by imposing initial and end conditions for a stride that are assumed to be known or measurable (VELTINK *et al.*, 2003). The algorithm was tested in extensive computer simulations based on synthetic trajectories that had been derived from the experimental waveforms collected in our current research on foot inertial sensing (SABATINI *et al.*, 2004).

2 Method

2.1 *Attitude and positioning estimation*

Consider a rigid body in space and define a co-ordinate system, the body frame $\mathcal{B}$, attached to the body. The problem of attitude estimation is to specify the orientation of the axes of $\mathcal{B}$ with respect to the reference co-ordinate system $\mathcal{R}$. The problem of positioning estimation is to specify the origin of $\mathcal{B}$ relative to $\mathcal{R}$. Suppose a vector $\vec{x}$ is resolved along the axes of $\mathcal{B}$ and $\mathcal{R}$, to yield the 3×1 column vectors $\vec{x}^b$ and $\vec{x}^r$, respectively. The attitude matrix $\boldsymbol{A}$ is the orthogonal matrix that brings the axes of $\mathcal{R}$ into the axes of $\mathcal{B}$, namely $\vec{x}^b = \boldsymbol{A}\vec{x}^r$.

A convenient representation of attitude is based on the 4×1 quaternion $\vec{q} = [q_0, \vec{e}^T]^T$ (from $\mathcal{R}$ onto $\mathcal{B}$), where q_0 is the scalar part, and $\vec{e} = [q_1, q_2, q_3]^T$ is the vector part; see the Appendix. The body angular motion can be described by the differential equation (CHOU, 1992)

$$\frac{d}{dt}\vec{q}(t) = \boldsymbol{\Omega}[\vec{\omega}(t)]\vec{q}(t) \tag{1}$$

where

$$\Omega[\vec{\omega}(t)] = \frac{1}{2}\begin{bmatrix} 0 & -\omega_z & \omega_y & \omega_x \\ \omega_z & 0 & -\omega_x & \omega_y \\ -\omega_y & \omega_x & 0 & \omega_z \\ -\omega_x & -\omega_y & -\omega_z & 0 \end{bmatrix} \tag{2}$$

is a 4×4 skew symmetrical matrix, constructed from the 3×1 vector $\vec{\omega}(t) = [\omega_x, \omega_y, \omega_z]^T$, the angular velocity of $\mathcal{B}$ relative to $\mathcal{R}$, resolved in $\mathcal{B}$.

The discrete-time model that describes the attitude kinematics is expressed by

$$\begin{cases} \vec{q}_{k+1} = \exp(\Omega_k T_s)\vec{q}_k & k = 0, 1, \ldots \\ \vec{q}_0 = \vec{q}(0) \end{cases} \tag{3}$$

The vector $\vec{q}_k$ is the quaternion at the time instant kT_s, where T_s is the system's sampling interval. Equation (3) is valid provided that the angular velocity $\vec{\omega}_k$ measured at the time instant kT_s is assumed to be constant in the time interval $[kT_s,(k+1)T_s]$. The process of computing the initial condition $\vec{q}_0$ is usually called alignment. Once (3) is solved, the attitude matrix can be updated

$$\boldsymbol{A}(\vec{q}) = (q_0^2 - \vec{e}^T\vec{e})\boldsymbol{I} + 2\vec{e}\vec{e}^T - 2q_0[\vec{e}\times] \tag{4}$$

where $\boldsymbol{I}$ is the 3×3 identity matrix and $[\vec{e}\times]$ is a skew symmetrical operator that represents the standard vector cross-product, see the Appendix.

The attitude estimate is used twice during positioning estimation. The accelerometer senses the body's own (non-gravitational) acceleration, $\vec{a}^b(t)$ as the superposition of the sensed acceleration in $\mathcal{B}$, $\vec{a}(t)$, and the projection of the gravitational acceleration $\vec{g}$ on $\mathcal{B}$

$$\vec{a}^b(t) = \vec{a}(t) - \boldsymbol{A}[\vec{q}(t)]\vec{g} \tag{5}$$

The next step requires integration of $\vec{a}^r(t) = \boldsymbol{A}[\vec{q}(t)]^T\vec{a}^b(t)$ to derive the position estimate

$$\vec{p}^r(t) = \int_0^t dt' \int_0^{t'} \boldsymbol{A}^T[\vec{q}(t'')]\vec{a}^b(t'')\,dt'' \tag{6}$$

A numerical integration routine such as the trapezoidal rule can be used to solve (6) numerically.

2.2 *Quaternion-based strap-down integration method*

A block diagram of the proposed strap-down integration method is depicted in Fig. 1.

In our approach to strap-down integration, the attitude estimate relies on the gyroscope when the body is in motion. Because of its sensitivity to both the gravity vector and the (non-gravitational) acceleration of the point where it is affixed, the accelerometer is used to estimate the static inclination of $\mathcal{B}$ relative to $\mathcal{R}$ when the body is stopped. As the rotation around the vertical cannot be sensed by the accelerometer, additional sensors would be necessary, e.g. a triaxial magnetometer, to sense the Earth's magnetic field (not considered here). Given these occasional gravity-orientation updates, the system can correct its gyroscope-induced orientation errors for an indefinite duration. This is an example of a 'zero velocity update' (VERPLAETSE, 1996).

In this respect, gait is ideal for application of a zero-velocity update. This is because a gait signal is cyclical, with periods of the order of seconds, and composed of different phases (VELTINK *et al.*, 1996): stance, including foot-flat, when the alignment can be performed, and swing, when the quaternion is time-propagated, according to (3), until the foot-flat of the next stride is detected. However, owing to the process of error build-up, the initial and end conditions of each stride can be different, in terms of both the orientation and the linear velocity of the involved leg segment. As for the attitude quaternion, the imposition of equal initial and end conditions can be achieved by applying the spherical linear interpolation (SLERP) procedure (SHOEMAKE, 1985). Let $T = MT_s$ be the foot-flat time instant when the integration of (3) is terminated. Let us introduce the error quaternion

$$\vec{q}^{\,e} = \vec{q}_0 \otimes \vec{q}_M^{\,-1} = [q_0^e, \vec{e}^{\,e}]^T \tag{7}$$

where $\otimes$ stands for the product operator associated with quaternions, see the Appendix. $\vec{q}_0$ and $\vec{q}_M$ are normalised before the SLERP procedure is applied to ensure they represent rotations on the unit sphere. $\vec{q}^{\,e}$ defines the transformation that aligns $\vec{q}_M$ into $\vec{q}_0$, explaining the rotational effect of the error build-up process. The SLERP procedure is applied as follows:

$$\begin{cases} \vec{q}_k^{\,i} = \dfrac{\vec{q}_0^{\,i} \sin[(1-\rho_k)\Omega] + \vec{q}^{\,e} \sin[\rho_k \Omega]}{\sin \Omega} \\ \vec{q}_0^{\,i} = [1, 0, 0, 0]^T \end{cases} \tag{8}$$

where $\rho_k = k/M$, $k = 0, \ldots, M$, and $\Omega = \arccos(q_0^e)$. The normalised quaternion $\vec{q}^{\,i}$ moves the unit sphere along an arc connecting $\vec{q}_0^{\,i}$ to $\vec{q}_M^{\,i} = \vec{q}^{\,e}$. Finally, the desired expression of the interpolated quaternion, which fulfils the initial and end conditions for a stride, is as follows:

$$\vec{q}_k^{\,u} = \vec{q}_k^{\,i} \otimes \vec{q}_k, \quad k = 0, \ldots, M \tag{9}$$

The gravity-compensated acceleration is then single time-integrated; the initial and end conditions are imposed to avoid drift (null velocity), before positioning estimation.

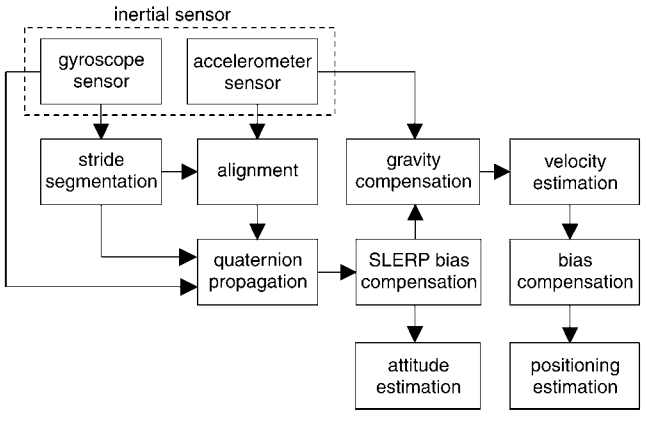

Fig. 1 *Flow-chart of whole strap-down integration algorithm*

2.3 *Movement trajectory*

An element of complication in the performance analysis of the strap-down integration algorithm is the effect that the sensed trajectory may have on its behaviour. It is well known that certain errors of the inertial sensors are trajectory-dependent (ABBOTT and POWELL, 1999). Henceforth, rather than on a wide variety of trajectories in three-dimensional space, the 3D strap-down integration method is exercised on a synthetic trajectory; the synthetic trajectory is intended to replicate, in the sense outlined below, important features of real walking trajectories.

The synthetic trajectory was constructed based on the following assumptions:

(*a*) the origin of $\mathcal{B}$ is where the IMU is located
(*b*) the trajectory of the origin of $\mathcal{B}$ reconstructed in $\mathcal{R}$, is embedded in the sagittal *X, Z*-plane: the co-ordinate axes *X*, *Y* and *Z* of $\mathcal{R}$ are directed in the anterior, medio-lateral and head directions, respectively
(*c*) the angular velocity vector is always oriented in the *Y*-direction
(*d*) the components of the linear velocity/acceleration expressed in $\mathcal{R}$, and the angular velocity are null in the time intervals from foot-flat to heel-off.

Underlying (*b*) and (*c*) is the modelling assumption that the leg motion is planar; (*d*) may be valid, depending on the choice of the sensed anatomical point (SABATINI *et al.*, 2004).

The simulations in this paper were carried on a 30 s long synthetic trajectory sampled at 200 Hz, which corresponds to a walking trial with the following features: stride time: 1.32 s; stride length: 1.10 m; relative stance: 63%. Three consecutive cycles of angular velocity and sagittal displacements are shown in Fig. 2. The synthetic trajectory was constructed from the time-normalised, ensemble-averaged waveforms of angular velocity and sagittal displacements of the foot instep, as they were reconstructed by a reduced-complexity IMU, composed of one biaxial accelerometer and one uniaxial gyroscope (SABATINI *et al.*, 2004).

In our simulations, the synthetic trajectory allowed us to define a true reference for computing the orientation/position estimation errors incurred by the 3D strap-down integration method; see Section 2.5. Furthermore, to produce the simulated sensed accelerations from data such as those appearing in Fig. 2, the angular velocity was numerically integrated, to yield the pitch angle; the displacements were then numerically differentiated twice, to yield the accelerations sensed in $\mathcal{R}$, and then in $\mathcal{B}$, provided that the pitch-dependent gravity contribution was properly accounted for in the procedure of signal construction. The pitch angle (pointing downward) was assumed to take a constant value during foot-flat, e.g. $-30°$; roll and yaw angles were null throughout the gait cycle (planar gait model). The synthetic trajectory was periodical with period D_{gait} (here, $D_{gait} = 1.32$ s), which implies that physiological stride variability was not simulated, e.g. by modulating the duration of each cycle or by submitting the waveform shapes to cycle-by-cycle changes.

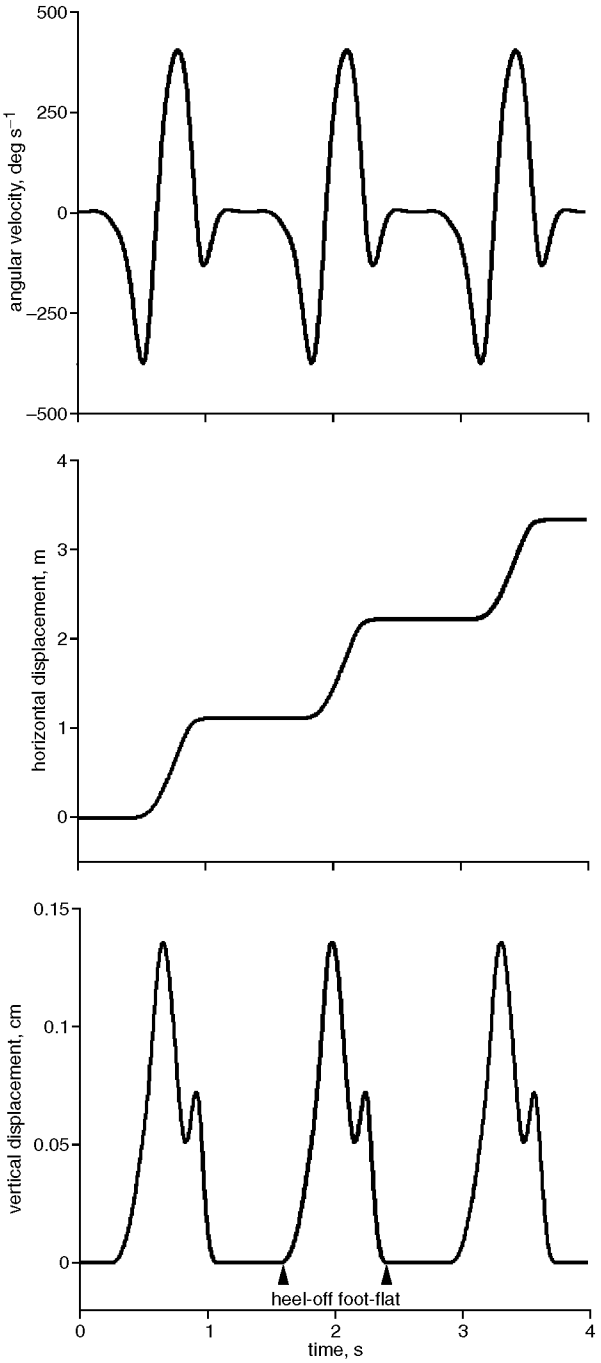

Fig. 2 *Time history of angular velocity, horizontal and vertical displacement: synthetic walking trial over interval lasting 4 s*

The procedure of gait phase detection implemented in the simulations was based on processing the Y-component of the signal from the simulated triaxial gyroscope. In particular, the procedure enabled the identification of the start time (heel-off detection) and the end time (foot-flat detection) to support the strap-down integration. The procedure was identical to the procedure implemented in SABATINI *et al.* (2004).

2.4 *Sensor models*

Both the gyroscope and the accelerometer were composed of sensor triplets, with their nominal sensitivity axes being mutually orthogonal. The gyroscope output $\vec{v}_g$ and the accelerometer output $\vec{v}_a$, in response to the angular velocity vector $\vec{\omega}$ and to the acceleration vector $\vec{a}$, both resolved in $\mathcal{B}$, are expressed by (FERRARIS *et al.*, 1995)

$$\begin{cases} \vec{v}_g = \boldsymbol{K}_g\vec{\omega} + \vec{o}_g + \vec{w}_g \\ \vec{v}_a = \boldsymbol{K}_a\vec{a}_m + \vec{o}_a + \vec{w}_a \end{cases} \tag{10}$$

where $\boldsymbol{K}_g = k_g\boldsymbol{I}$, $\boldsymbol{K}_a = k_a\boldsymbol{I}$ are the matrices of the scale factors; the sensors are assumed to be identical; $\vec{o}_g, \vec{o}_a$ are the bias vectors; and $\vec{w}_g, \vec{w}_a$ are white Gaussian measurement noise vectors, with null mean and covariance matrix $\boldsymbol{C}_g = \sigma_g^2\boldsymbol{I}$ and $\boldsymbol{C}_a = \sigma_a^2\boldsymbol{I}$, respectively. Uncertainty sources, such as cross-axis sensitivity, cross-coupling coefficients and misalignment are not modelled in (10).

It is known that the scale factors and biases of inertial sensors are functions of environmental conditions, i.e. ambient temperature, and are highly dependent on the characteristics of individual devices. Although thermal modelling was not performed here in the true sense, some essential aspects of the behaviour of a representative IMU were captured over a limited temperature range. First, as extreme temperatures were avoided, the assumption that the scale factor and bias vary linearly with the temperature was approximately valid: a non-linear model was assumed to describe the thermal variations of the gyroscope bias. Secondly, the gyroscope bias was known to depend strongly on time and temperature (BARSHAN and DURRANT-WHYTE, 1994). However, the time dependence was indirectly due to temperature variations, i.e. the component self-heating at system start-up (ABBOTT and POWELL, 1999): here, the time dimension was discarded by assuming that steady-state conditions were reached at each temperature before the simulated walking trial was started.

The inertial sensors were assumed to be perfectly calibrated at the reference temperature $T_{ref} = 25°C$ (null bias; $k_g = 4\ \text{mV}^{\circ-1}\text{s}^{-1}$; $k_a = 100\ \text{mV}g^{-1}$; the gravitational acceleration was $g = 9.81\ \text{ms}^{-2}$). The difference between the environment temperature and T_{ref}, henceforth called thermal mismatching, was explored by taking steps of 5°C from a minimum temperature $T_{min} = 15°C$ to a maximum temperature $T_{max} = 35°C$, see Fig. 3. As for the gyroscope (MURATA, 1999), the bias was assumed to change from $8°\text{s}^{-1}$ at T_{min}, to $0°\text{s}^{-1}$ at T_{ref}, to $-15°\text{s}^{-1}$ at T_{max}, yielding, at first approximation, data similar to those reported in PAPPAS *et al.* (1999); the scale factor was assumed to change within a range of $\pm 5\%$ over the range $[T_{min}, T_{max}]$. As for the accelerometer (ANALOG DEVICES, 1999), the $0g$ bias against temperature was assumed to be $2\ \text{mg}°\text{C}^{-1}$, and the temperature drift of the

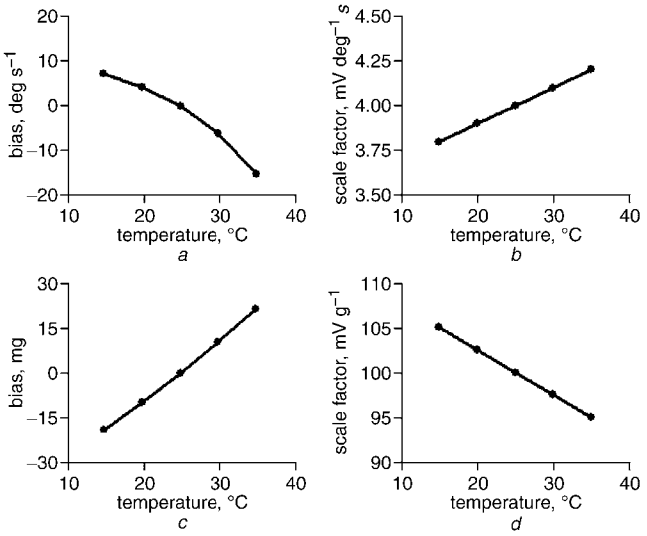

Fig. 3 *Behaviour of bias and scale factor as function of temperature for (a), (b) simulated gyroscope and (c), (d) accelerometer*

scale factor was $\pm 5\%$ over the range $[T_{min}, T_{max}]$. Depending on the measurement noise level, three IMUs were simulated: noiseless IMU; high-quality IMU: $\sigma_g = 0.5^{\circ}s^{-1}$, $\sigma_a = 1$ mg; and fair-quality IMU: $\sigma_g = 2.5^{\circ}s^{-1}$, $\sigma_a = 5$ mg.

2.5 *Performance metrics*

The accuracy of the attitude estimation is based on computing $\Delta\vec{q} = \vec{q}_t^{-1} \otimes \vec{q}_{est}$, where $\vec{q}_t$ and $\vec{q}_{est}$ are the true and estimated quaternions, respectively. $\vec{q}_t$ is easily computed by feeding the samples of the true angular velocity (see Fig. 2) to (3); $\vec{q}_{est}$ is produced by the strap-down integration algorithm itself. The unit-length quaternion $\Delta\vec{q}$ represents the rotation that brings the estimated body frame onto $\mathcal{B}$. The orientation error is obtained from the scalar component of $\Delta\vec{q}$:$\Delta\theta = 2\arccos(\Delta q)$. The performance metrics are given by the RMS value of the orientation error $\Delta\theta$ ($RMSE_\theta$), and by the RMS value of the magnitude of the three-dimensional displacement error between the true trajectory and the reconstructed trajectory ($RMSE_d$).

3 Results

Monte Carlo simulations were carried out to test the efficacy of the SLERP procedure, i.e. SLERP and NO-SLERP, and to assess the influence of the duration of the integration interval D, i.e. $D = D_{gait}$ (single-cycle update); $D = 2D_{gait}$ (double-cycle update). All four combinations were tested for different temperatures and measurement noise levels. Three simulation sets were considered: for both sensors, the bias and the scale factor values at temperatures other than T_{ref} were erroneously considered identical to the values corresponding to the temperature T_{ref} (set 1); see Figs 4 and 5.

Conversely, the sensor parameters, i.e. bias and scale factor, were assumed to be accurately estimated at each ambient temperature for the accelerometer, whereas the gyroscope was subject to the effects of thermal mismatching (set 2); see Figs 6 and 7.

Finally, the gyroscope parameters were assumed to be accurately estimated at each ambient temperature, whereas the accelerometer parameters were those evaluated at T_{ref} in the simulations whose results are reported in Figs 8 and 9 (set 3).

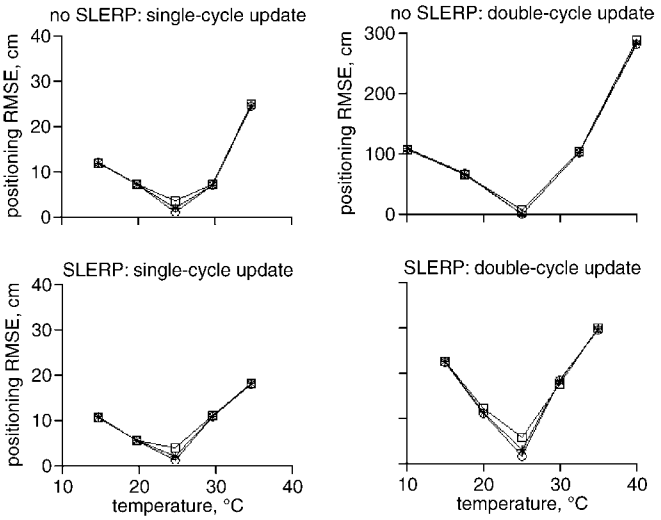

Fig. 5 *Positioning RMSE: results of simulation experiments (set 1): (○) noiseless IMU; (∗) high-quality IMU; (□) fair-quality IMU*

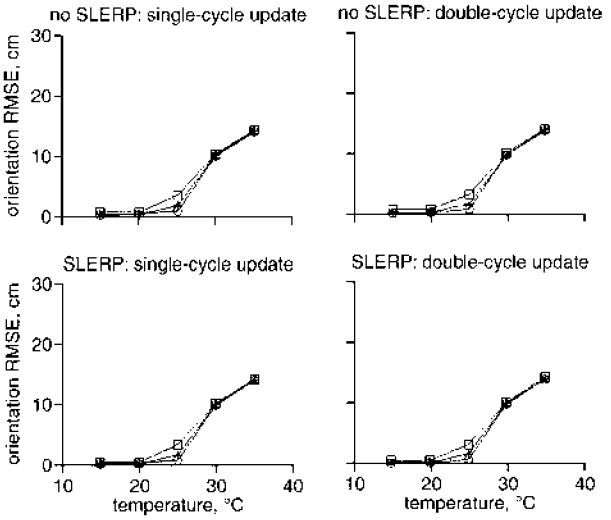

Fig. 6 *Orientation RMSE: results of simulation experiments (set 2): (○) noiseless IMU; (∗) high-quality IMU; (□) fair-quality IMU*

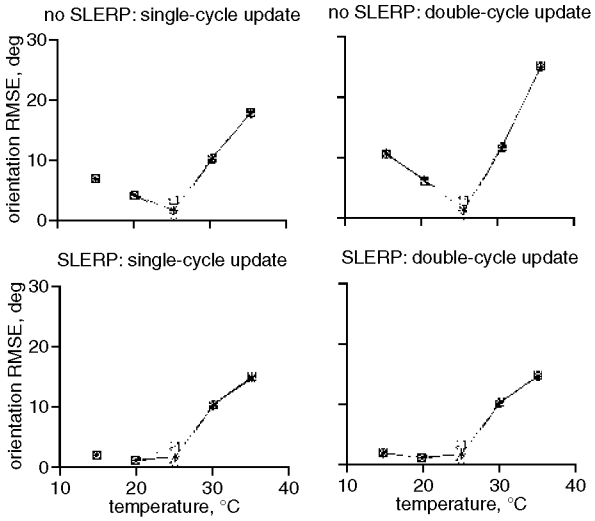

Fig. 4 *Orientation RMSE: results of simulation experiments (set 1): (○) noiseless IMU; (∗) high-quality IMU; (□) fair-quality IMU*

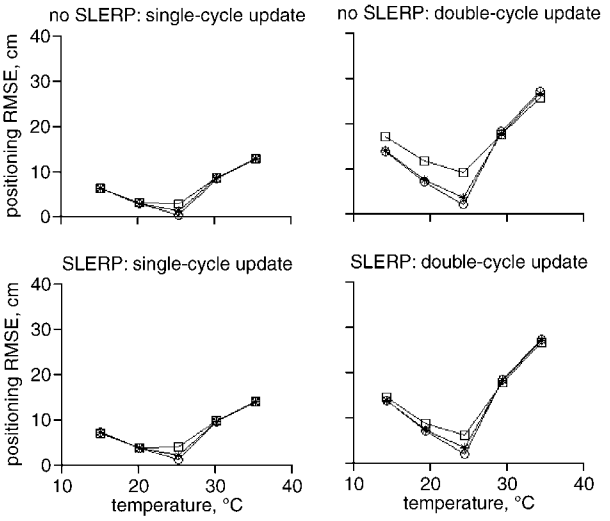

Fig. 7 *Positioning RMSE: results of simulation experiments (set 2): (○) noiseless IMU; (∗) high-quality IMU; (□) fair-quality IMU*

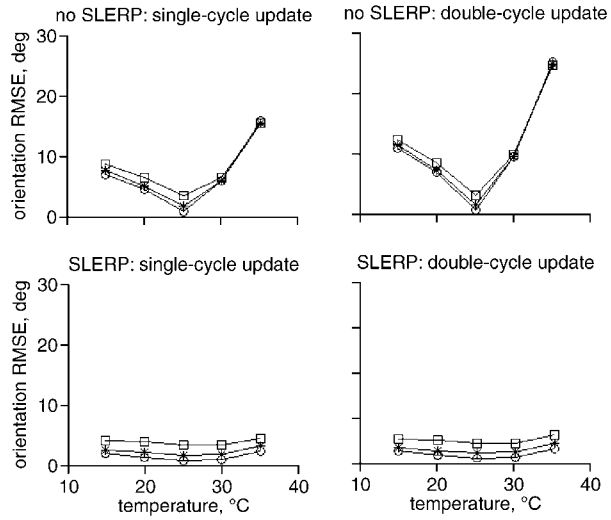

Fig. 8 *Orientation RMSE: results of simulation experiments (set 3): (○) noiseless IMU; (∗) high-quality IMU; (□) fair-quality IMUl*

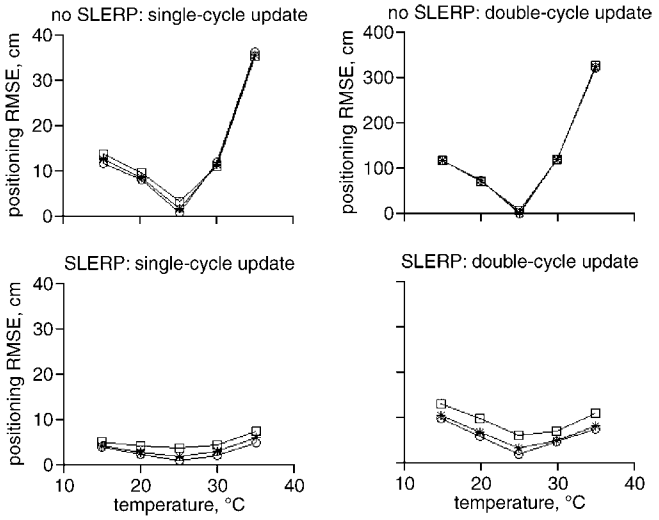

Fig. 9 *Positioning RMSE: results of simulation experiments (set 3): (○) noiseless IMU; (∗) high-quality IMU; (□) fair-quality IMU*

4 Discussion and conclusions

When the inertial sensors work at the ambient temperature T_{ref}, $RMSE_\theta < 0.83^\circ$ and $RMSE_d < 0.90$ cm (noiseless IMU); $RMSE_\theta < 3.30^\circ$ and $RMSE_d < 3.53$ cm (fair-quality IMU), for the SLERP–single-cycle update combination. When the scale factor and bias values are accurate, applying the SLERP procedure is not relevant; also, the performance is minimally degraded if the duration of the integration interval doubles. The errors when the noiseless IMU is at T_{ref} are due to the effect of thresholding by the stride segmentation procedure; the threshold values are matched to the maximum value expected for the gyroscope bias and left unchanged throughout the entire simulation session.

The influence of thermal mismatching on the attitude and positioning estimation process in the set 1 simulations is greater than the impact of the measurement noise alone, in particular when the ambient temperature is higher than T_{ref}. The RMSE curves are generally not symmetrical around T_{ref} because of the particular model, which explains the functional dependence of the inertial sensors' bias and scale factor drift on the temperature: the non-linear model for the gyroscope bias emphasises, in particular, the bias magnitude when the temperature is higher than T_{ref}. The influence of thermal mismatching is greatly attenuated by the SLERP procedure: an improvement of up to 3° (single-cycle update) and 11° (double-cycle update) in the accuracy of orientation estimates was observed at $T_{max} = 35^\circ$C. The SLERP procedure is greatly beneficial to the double integration process as well, yielding up to a tenfold improvement in the accuracy of the positioning estimate (single-cycle update compared with double-cycle update).

When the gyroscope is not perfectly calibrated (set 2), $RMSE_\theta$ is almost constant in the range of tested temperatures after the SLERP procedure has been applied, and it is not substantially affected by the duration of the integration interval. Compared with the NO-SLERP–double-cycle update combination, the performance improvement is remarkable. It is the effect of the error in the alignment process that cannot be eliminated by the SLERP procedure; the initial error, indeed, does not depend on the ambient temperature for a perfectly calibrated accelerometer. Because of the action of the SLERP procedure, there exists a significant improvement in the accuracy of the positioning estimates, especially in the case of a double-cycle update.

When the accelerometer is not perfectly calibrated (set 3), there exist no benefits in applying the SLERP procedure, for either the single-cycle or double-cycle update. This makes sense because the SLERP procedure does not correct for alignment errors; in the present case, the magnitude of the alignment errors increases with the amount of thermal mismatching. $RMSE_\theta$ in the set 3 simulations is less than $RMSE_\theta$ in the set 1 simulations at each tested temperature, as there exists a cumulative effect of the alignment errors and the gyroscope's imperfect calibration in the set 1 simulations. No benefits of the SLERP procedure are accrued to the positioning estimates, the accuracy of which is markedly dependent on the duration of the integration interval.

From all the simulation results presented, the performance sensitivity to the measurement noise level seems not to be critical. One of the most critical factors affecting the performance of the strap-down integration method is represented by the imperfect compensation for the gravity field in the accelerometer signals (FERRARIS *et al.*, 1995). Also, the simulation results highlight the critical role played by the gyroscope bias on the results of the whole strap-down algorithm because of its time integration during the estimation of the body orientation; as would be expected, the bias has the effect of restricting the time of accurate measurement. An important role is also played by the accelerometer bias, because of the induced alignment errors and the time-integrated uncertainty that affects the velocity and position estimates. Conversely, the uncertainties in the inertial sensors' scale factors are proportional to the current values of these quantities, as they are not time-integrated. Not shown here are the effects of the uncertainties in the scale factor values, which are smaller than those due to the uncertainties in the bias values.

The analysed $RMSE_\theta$ does not include the contribution due to the inability of the accelerometer to estimate heading. In this paper, the yaw angle was estimated to be zero, as we assume that we know the characteristics of the tracked movement. One way to overcome this sensing limitation is by integrating additional sensors in the IMU, e.g. a triaxial magnetometer. As this sensor is insensitive to gravity, its integration allows us to perform measurement updates during swing. In the present approach, the alignment process is a sort of measurement update that is carried out during stance. This is because we are not in a position to discriminate between gravitational components and acceleration components due to body motion in the accelerometer signals, unless the movement is sufficiently slow, a condition that is difficult to define, especially when the sensed anatomical point is on the leg (VELTINK *et al.*, 1996; WU and LADIN, 1996; SABATINI *et al.*, 2004).

During stance, the quaternion can be considered steady: its (optimum) estimate can be derived from averaging the inclination estimate over a number of measurement samples. These measurement samples would also be used to implement procedures for in-use calibration, yielding the bias and scale factor of accelerometers (LÖTTERS *et al.*, 1998) and the bias of gyroscopes (WILLIAMSON and ANDREWS, 2001); in principle, these procedures could be considered in association with the SLERP procedure. The difficulty in defining a set of rotations of the body-mounted IMU complicates the in-use calibration of the scale factor of gyroscopes, as discussed in FERRARIS *et al.* (1995).

Once the alignment process is terminated, the system dynamics during the swing phase is time-propagated without any further measurement update occurring 'during the flight'. Planned developments involve including triaxial magnetometers in the simulated scenario and implementing quaternion-based Kalman filtering algorithms to perform the strap-down integration process.

Acknowledgment—This work has been supported in part by funds from the Italian Ministry of University and Research.

Appendix

A popular attitude representation is the quaternion $\vec{q} = [q_0, q_1, q_2, q_3]^T$, a real 4×1 column-vector composed of a scalar part $q = q_0$ and a vector part $\vec{e} = q_1\vec{i} + q_2\vec{j} + q_3\vec{k}$. In turn, q_1, q_2, q_3 are scalar values, and $\vec{i}, \vec{j}, \vec{k}$ are symbolic elements that are defined as follows: $\vec{i} = [0, 1, 0, 0]^T$, $\vec{j} = [0, 0, 1, 0]^T$, $\vec{k} = [0, 0, 0, 1]^T$; in a sense, quaternions can be considered an extension of complex numbers that define a four-dimensional volume by means of one 'real' element, the scalar part, and three 'imaginary' elements, the vector part. An alternative form for representing a quaternion is

$$\vec{q} = [q, \vec{e}] \tag{11}$$

which allows us to simplify the expression of the quaternion product, associated with the quaternions and denoted by $\otimes$

$$\vec{q}_a \otimes \vec{q}_b = [q_a q_b - \vec{e}_a \cdot \vec{e}_b,\ q_a\vec{e}_b + q_b\vec{e}_a + \vec{e}_a \times \vec{e}_b] \tag{12}$$

where $(\cdot)$ stands for the standard vector dot product, and $(\times)$ stands for the standard vector cross product.

The norm of the quaternion is defined as follows:

$$|\vec{q}| = \sqrt{q^2 + |\vec{e}|^2} \tag{13}$$

where $|\vec{e}| = \sqrt{q_1^2 + q_2^2 + q_3^2}$ is the norm of the vector $\vec{e}$, intended in the Euclidean sense. Unit quaternions are characterised by unit norm. It is straightforward to demonstrate that the product of two unit quaternions is also of unit norm. Finally, the multiplicative inverse $\vec{q}^{-1}$ of the quaternion $\vec{q}$ is defined as follows:

$$\vec{q}^{-1} = \left[\frac{q}{q^2 + |\vec{e}|^2},\ \frac{-\vec{e}}{q^2 + |\vec{e}|^2}\right]. \tag{14}$$

The interest for quaternions comes from the observation that unit quaternions can always be put in the form

$$\vec{q} = \left[\cos\left(\frac{\theta}{2}\right), \sin\left(\frac{\theta}{2}\right)\vec{u}\right] \tag{15}$$

where $|\vec{u}| = 1$.

The rotation of an ordinary vector $\vec{p}$ by a quaternion $\vec{q} = [\cos(\theta/2), \sin(\theta/2)\vec{u}]$ is defined as $\vec{p}_{\text{rot}} = \vec{q} \otimes [0, \vec{p}]^T \otimes \vec{q}^{-1}$; hence, $\vec{u}$ is a unit vector about which the vector $\vec{p}$ is rotated through an angle θ. The quaternion counterparts are thus the rotational axis and the rotational angle that are invoked in the Euler theorem on finite rotations. An interesting connection with the attitude matrix can be made by writing the relationship $\vec{x}^b = A\vec{x}^r$, (see Section 2) in the equivalent form

$$\vec{x}^b = \vec{q}^{-1} \otimes \vec{x}^r \otimes \vec{q} \tag{16}$$

($\vec{q}$ is from $\mathcal{R}$ onto $\mathcal{B}$). Finally, straightforward algebraic manipulations allow us to demonstrate (4); remember that, in (4), the skew symmetrical operator $[\vec{e}\times]$ has the following expression:

$$[\vec{e}\times] = \begin{bmatrix} 0 & -e_z & e_y \\ e_z & 0 & -e_x \\ -e_y & e_x & 0 \end{bmatrix} \tag{17}$$

References

ABBOTT, E., and POWELL, D. (1999): 'Land-vehicle navigation using GPS', *Proc. IEEE*, **87**, pp. 145–162

AMINIAN, K., REZAKHANLOU, K, ANDRES, E. D., FRITSCH, C., LEVYRAZ, P.-F., and ROBERT, P. (1999): 'Temporal feature estimation during walking using miniature accelerometers: an analysis of gait improvement after hip arthroplasty', *Med. Biol. Eng. Comput.*, **37**, pp. 686–691

AMINIAN, K., NAJAFI, B., BÜLA, C., LEVYRAZ, P.-F., and ROBERT, P. (2002): 'Spatio-temporal parameters of gait measured by an ambulatory system using miniature gyroscopes', *J. Biomech.*, **35**, pp. 689–699

ANALOG DEVICES, INC. (1999): 'ADXL210E Technical Data Sheet'. http://www.analog.com

BACHMANN, E. R. (2000): 'Inertial and magnetic tracking of limb segment orientation for inserting humans in synthetic environments'. PhD thesis, Naval Postgraduate School, Monterrey, CA, USA

BARSHAN, B., and DURRANT-WHYTE, H. F. (1994): 'Evaluation of a solid-state gyroscope for robotics applications', *IEEE Trans. Instrum. Meas.*, **44**, pp. 61–67

BORTZ, J. E. (1971): 'A new mathematical formulation for strapdown inertial navigation', *IEEE Trans. Aerosp. Elec. Syst.*, **7**, pp. 61–66

BUSSMANN, J. B. J., VELTINK, P. H., KOELMA, F., VAN LUMMEL, R. C., and STAM, H. J. (1995): 'Ambulatory monitoring of mobility-related activities: the initial phase of the development of an activity monitor', *Eur. J. Phys. Med. Rehab.*, **5**, pp. 2–7

CHOU, J. C. K. (1992): 'Quaternion kinematic and dynamic differential equations', *IEEE Trans. Rob. Automat.*, **8**, pp. 53–64

FERRARIS, F., GRIMALDI, U., and PARVIS, M. (1995): 'Procedure for effortless in-field calibration of three-axis rate gyros and accelerometers', *Sensors Mater.*, **7**, pp. 311–330

GUILLEMAUD, R., CARITU, Y., DAVID, D., FAVRE-RÉGUILLON, F., FONTAINE, D., and BONNET, S. (2003): 'Body motion capture for activity monitoring'. *Int. Workshop on New Generation of Wearable Systems for eHealth*, Dec. 11–14, Castelvecchio Pascoli, Lucca, Italy

KIRTLEY, C. (2001): 'Summary: Quaternions vs. Euler angles'. BIOMCH-L Discussion, May 3, 2001, http://isb.ri.ccf.org/biomch-l/archives/biomch-l-2001-05

LÖTTERS, J. C., SCHIPPER, J., VELTINK, P. H., OLTHIUS, W., and BERGVELD, P. (1998): 'Procedure for in-use calibration of triaxial accelerometers in medical applications', *Sensors Actuators A*, **68**, pp. 221–228

LUINGE, H. J. (2002): 'Inertial sensing of human movement'. PhD thesis, University of Twente, Twente University Press, Enschede, The Netherlands

MAYAGOITIA, R. E., NENE, A. V., and VELTINK, P. H. (2002): 'Accelerometer and rate gyroscopes measurement of kinematics: an inexpensive alternative to optical motion analysis systems', *J. Biomech.*, **35**, pp. 537–542

MIYAZAKI, S. (1997): 'Long-term unrestrained measurement of stride length and walking velocity utilizing a piezoelectric gyroscope', *IEEE Trans. Biomed. Eng.*, **44**, pp. 753–759

MURATA MANUFACTURING CO., LTD. (1999): 'Data sheet of Gyrostar® Model: ENC-03JA ENC-03JB', http://www.murata.com

OHTAKI, Y., SAGAWA, K., and INOOKA, H. (2001): 'A method for gait analysis in a daily living environment by body-mounted instruments', *JSME Int. J.*, **44**, pp. 1125–1132.

PAPPAS, I. P. I., KELLER, T., and POPOVIC, M. R. (1999): 'Experimental evaluation of the gyroscope sensor used in anew gait phase detection system', *Proc. 4th Ann. Conf. Int. Functional Electrical Stimulation Society*, August 23–27, Sendai, Japan, pp. 12–16

PAPPAS, I. P. I., POPOVIC, M. R., KELLER, T., DIETZ, V., and MORARI, M. (2001): 'A reliable gait phase detection system', *IEEE Trans. Rehab. Eng.*, **9**, pp. 113–125

SABATINI, A. M., MARTELLONI, C., SCAPELLATO, S., and CAVALLO, F. (2004): 'Assessment of walking features from foot inertial sensing', *IEEE Trans. Biomed. Eng.*, in press

SHOEMAKE, K. (1985): 'Animating rotations with quaternion curves'. *Proc. SIGGRAPH 85*, ACM Press, pp. 245–254

VELTINK, P. H., BUSSMANN, H. B. J., DE VRIES, W., MARTENS, W. L. J., and VAN LUMMEL, R. C. (1996): 'Detection of static and dynamic activities using uniaxial accelerometers', *IEEE Trans. Rehab. Eng.*, **4**, pp. 375–385

VELTINK, P. H., SLYCKE, P., HEMSSEMS, J., BUSCHMAN, R., BULSTRA, G., and HERMENS, H. (2003): 'Three dimensional inertial sensing of foot movements for automatic tuning of a two-channel implantable drop-foot stimulator', *Med. Eng. Phys.*, **25**, pp. 21–28

VERPLAETSE C. (1996): 'Inertial proprioceptive devices: self-motion-sensing toys and tools', IBM Systems Journal, **35**(3–4), pp. 639–650

WILLIAMSON, R., and ANDREWS, B. J. (2001): 'Detecting absolute human knee angle and angular velocity using accelerometers and gyroscopes', *Med. Biol. Eng. Comput.*, **39**, pp. 294–302

WU, G., and LADIN, Z. (1996): 'The study of kinematic transients in locomotion using the integrated kinematic sensor', *IEEE Trans. Rehab. Eng.*, **4**, pp. 193–200

Author's biography

ANGELO M. SABATINI received the Dr. Eng. degree in electrical engineering from the University of Pisa, Italy in 1986, and the PhD degree in biomedical robotics from Scuola Superiore Sant'Anna, Pisa in 1992. From 1987–1988 he was with Centro E. Piaggio, Faculty of Engineering, University of Pisa. During the summer of 1988 he was a visiting scientist at the Artificial Organ Lab, Brown University, Providence, RI, U.S.A. From 1991–2001 he was an assistant professor of biomedical engineering at Scuola Superiore Sant'Anna, where he has been an associate professor of biomedical engineering since 2001. His main research interests are: design and validation of intelligent assistive devices and wearable sensor systems, biomedical signal processing and quantification of human performance.